Corrosion Resistance of Cold-Spray Ni and Ti Coatings under Chloride-Containing Conditions

Jeongjun Lee [a], Jinwook Choi [a], Hwasung Yeom [a*]
[a] *Pohang University of Science and Technology (POSTECH), Pohang-Si, Gyeongsangbuk-do, South Korea*
[*] *Corresponding author: hyeom@postech.ac.kr*

Keywords : Spent nuclear fuel (SNF), Stress corrosion cracking (SCC), cold spray coating

1. Introduction

With the increasing emphasis on carbon neutrality, nuclear energy has emerged as a prominent low-carbon power source. Nonetheless, one of its fundamental challenges for nuclear energy is the management of spent nuclear fuel, which raises concerns regarding the long-term sustainability of nuclear power generation. Although deep geological disposal represents a potential long-term solution, most countries currently depend on interim storage methods, including wet storage and dry cask storage systems. Wet storage facilities, however, are approaching the capacity limits. While dry cask storage systems have demonstrated structural robustness during extreme events such as the Fukushima accident, they still pose a susceptibility to long-term degradation in coastal environments due to salt-rich atmospheres.

Over extended periods, salt deposition on container surface in humid conditions can form brine, thereby initiating stress corrosion cracking (SCC) on the surface of stainless steel canisters. SCC arises from the simultaneous presence of tensile stress, a corrosive medium, and a susceptible material, as such the welded regions of canisters identified as particularly vulnerable regions [1].

This study investigates the application of cold spray coatings as a mitigation strategy for SCC in welded zones of stainless steel dry storage canisters. The cold spray process deposits metallic layers at relatively low temperatures, thus avoiding oxidation and phase transformations. Furthermore, the process introduces beneficial compressive stresses that counteract tensile stresses around the welded regions and establishes a protective barrier against chloride ingress. Overall, these effects enhance the long-term structural integrity and corrosion resistance of dry cask storage canisters.

2. Methods and Results

This section describes the sample preparation, followed by results that compare the corrosion resistance of the deposited materials.

2.1. Substrate Material

Square, flat stainless steel 304 (SS304) substrates (30 mm × 30 mm × 3 mm) were subjected to heat treatment at 650 ℃ for 48 hours in air in order to simulate the microstructural characteristics of the heat-affected zone (HAZ) typically observed in the welded regions of canisters employed in dry cask storage systems.

2.2 Coating Preparation

Ni and Ti coatings were deposited using a commercial cold spray system. The cold spray setup comprised an industrial robotic system, a converging–diverging nozzle, a gas preheater, and a powder feeding unit. Nitrogen was employed as the propellant gas.

Other deposition parameters, including spraying distance, nozzle transverse speed, feed rate, and spray angle, were maintained constant throughout the process.

To assess the effects of coating material and surface condition on corrosion behavior, the samples were divided into two groups. The first group consisted of three samples: bare SS304, Ni coated and Ti coated samples with surface polishing. The second group comprised samples with Ni and Ti as-sprayed condition. Ni and Ti were selected as coating materials due to their low galvanic corrosion tendency when coupled with stainless steel [2], as well as their intrinsic corrosion resistance. All sample surfaces were subsequently polished to a 1200-grit finish using SiC abrasive paper to remove surface oxides and ensure consistency in surface preparation.

Fig. 1. presents the surfaces of polished SS304, as-sprayed and polished coated samples. Metallic reflective surfaces are observed in Fig. 1a, 1b, and 1c, whereas Fig. 1d and 1e exhibit relatively dull appearances.

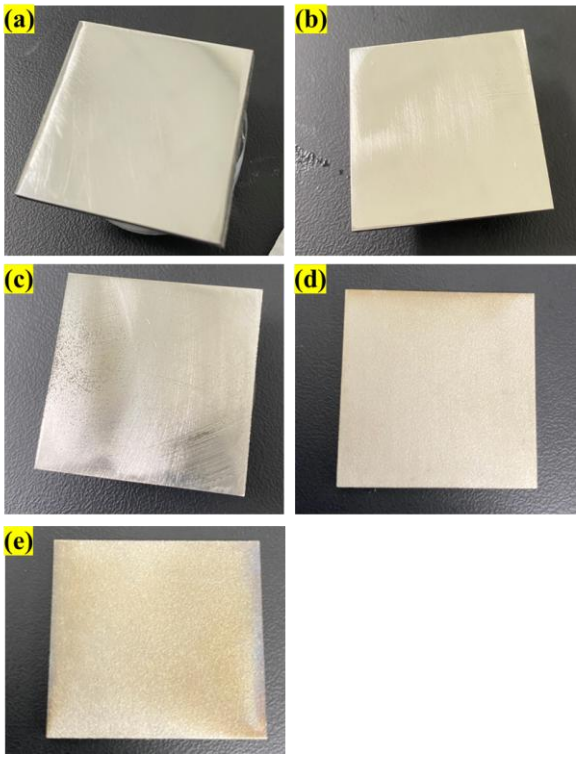

Fig. 1. Prepared sample images of of (a) Polished SS304 (b) Polished Ni (P-Ni) (c) Polished Ti (P-Ti) (d) Non-polished Ni (NP-Ni) (e) Non-polished Ti (NP-Ti)

The resulting surface roughness (R_a) values were measured using a 3D measuring laser microscope LEXT OLS5100 (OLYMPUS, Japan), approximately 0.42 ± 0.23 µm for SS304, 0.42 ± 0.30 µm for P-Ni, and 0.67 ± 0.11 µm for P-Ti. The surface roughness (R_a) of the as-deposited coatings was measured as 5.34 ± 0.48 µm for NP-Ni and 10.15 ± 2.68 µm for NP-Ti.

As shown in Fig. 2, the surface morphology differences are clearly confirmed by the 3D surface roughness images. Minimal variation is observed among the polished samples (Fig. 2a–c). In contrast, pronounced roughness differences are evident in Fig. 2d and particularly in Fig. 2e, where the surface irregularities are most severe.

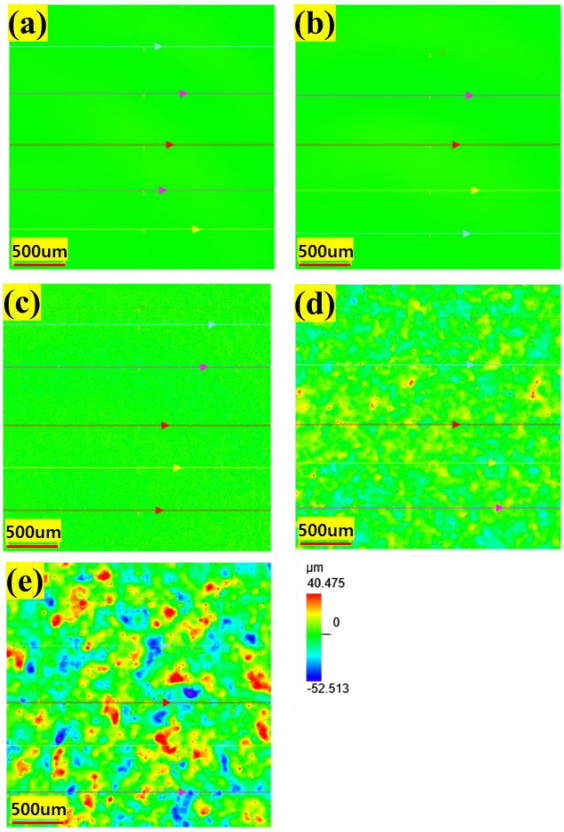

Fig. 2. Surface roughness 3D image of (a) SS304 (b) P-Ni (c) P-Ti (d) NP-Ni (e) NP-Ti

The coated substrates were sectioned into 1 cm × 1 cm specimens and cleaned with acetone in an ultrasonic bath, followed by air drying. The samples were subsequently mounted, ground, and polished. Microstructural characterization was performed using a JSM–7100F Scanning Electron Microscope (SEM, JEOL, Japan) equipped with an energy-dispersive X-ray spectroscopy (EDS) system and a backscattered electron detector, operated at 15 kV.

As shown in Fig. 3, strong bonding is evident both at the coating–substrate interface and at coating itself, attributed to the severe plastic deformation of powders upon impact.[3] No metallic oxides, cracks, or interconnected porosity were detected either at the interface or throughout the coating thickness.

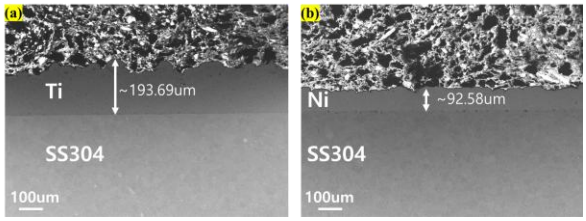

Fig. 3. Cross-sectional SEM image of cold spray coated samples: (a) Ti coating (b) Ni coating on sensitized SS304 substrate.

The average coating thicknesses were 194 µm for NP-Ti and 93 µm for NP-Ni. The surface morphology shown in Fig. 3 is consistent with the previously measured as-deposited roughness values (R_a) and with the

observations in Fig. 2, where the NP-Ti coating exhibits a comparatively rougher surface than the NP-Ni coating.

Optical Microscopy (OM) images were acquired using an OLYMPUS BX53MRF microscope to examine the sample morphology in detail before and after the corrosion tests. Fig. 4 shows OM images of the sample surfaces before corrosion test. In Fig. 4a, 4b and 4c, scratches from SiC polishing abrasive paper are visible, although the overall surface appears much smoother compared to the as-deposited samples shown in Fig. 4d and 4e. In Fig. 4c, the Ti-coated surface exhibits a brownish color, which is attributed to the formation of a TiO_2 film [3]. The rough surfaces in Fig. 4d and 4e are due to the presence of deposited powders.

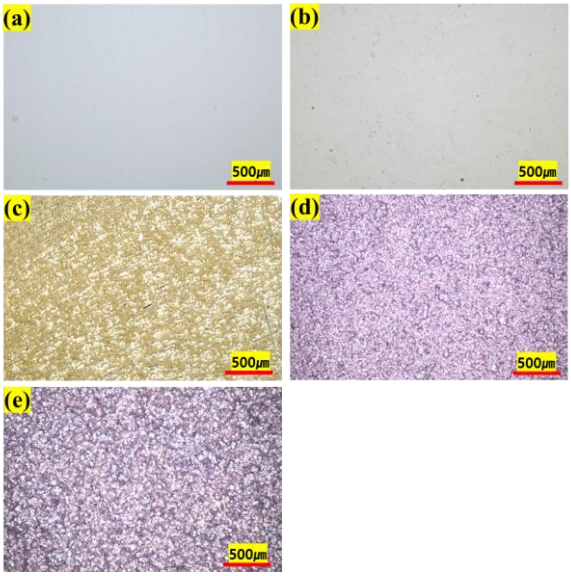

Fig. 4. OM image of the samples before corrosion test. (a) SS304 (b) P-Ni (c) P-Ti (d) NP-Ni (e) NP-Ti

The elemental line scan analyses for cross-sections of the coated samples are presented in Fig. 5. Fig. 5a and 5b show SEM images of NP-Ti and NP-Ni, respectively. Fig. 5c and 5d display the corresponding EDS line scan results. In the Ti-coated sample, Ti is dominant element in the coating region. The transition from the substrate to the coating is sharp, with no evidence of a significant diffused interface at the substrate/coating boundary. Similarly, in the Ni-coated sample (Fig. 5d), Ni is the main element detected in the coating, and a sharp transition is again observed, confirming that no diffused interface is formed.

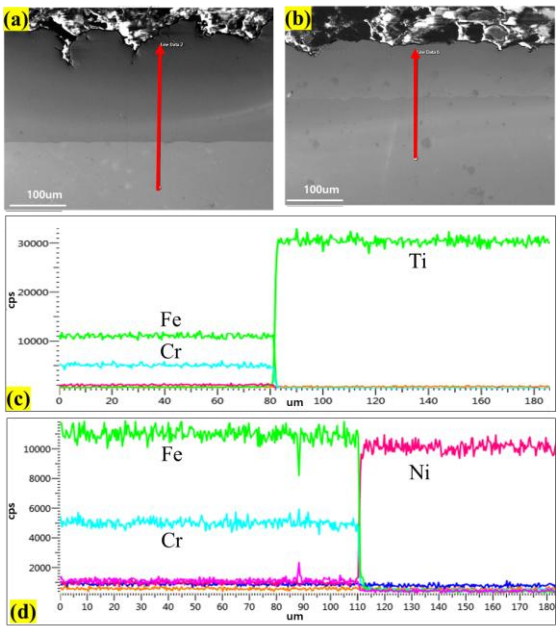

Fig. 5. SEM images of (a) NP-Ti and (b) NP-Ni showing the line scan direction. (c) EDS line scan analysis of (a), and (d) EDS line scan analysis of (b).

2.3 $FeCl_3$ corrosion test

Full immersion pitting tests were performed in accordance with ASTM G48, Method A. The sides and bottom surfaces of the specimens were coated with a rust-preventive spray, leaving only the major surface (15 mm × 15 mm) exposed to the corrosive media. The specimens were then immersed in a 6 wt.% ferric chloride solution at 22 °C for 72 h. After testing, the samples were rinsed with deionized water and dried with air. OM images were subsequently acquired to examine the morphology of the corrosion damage in detail.

Fig. 6 presents photographs of the samples after the $FeCl_3$ corrosion test. The uncoated sample (Fig. 6a) retains some surface brightness; however, pronounced blistering is evident. The polished Ni-coated sample (Fig. 6b) exhibits a marked reduction in brightness compared to its pre-test condition, whereas the polished Ti-coated sample (Fig. 6c) maintains its integrity, showing little to no change in surface appearance. In contrast, the as-deposited samples (Figs. 6d and 6e) display slight discoloration but no significant evidence of coating degradation or exposure.

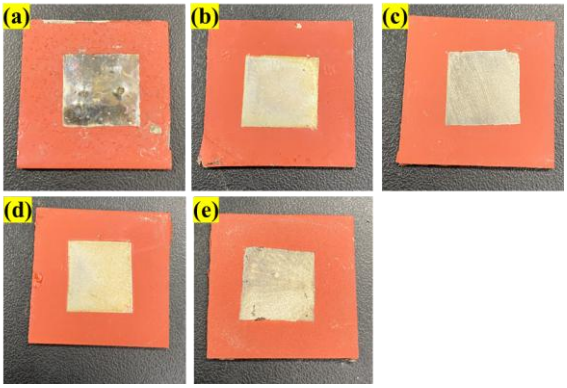

Fig. 6. Photographs of the samples after $FeCl_3$ corrosion test. (a) SS304 (b) P-Ni (c) P-Ti (d) NP-Ni (e) NP-Ti

Fig. 7 presents OM images of the sample surfaces after the $FeCl_3$ corrosion test. As shown in Fig. 6a, numerous surface defects are evident on the uncoated sample, consistent with the severe corrosion observed in Fig. 7a, indicating extensive surface attack by the $FeCl_3$ solution. In Fig. 7b, pronounced corrosion, particularly around the particle-particle boundaries is observed, in a good agreement with previous reports [4]. By contrast, corrosion-induced defects are scarcely visible in Fig. 7c. In Fig. 7d and 7e, the severe surface roughness makes it difficult to clearly identify distinct signs of corrosion.

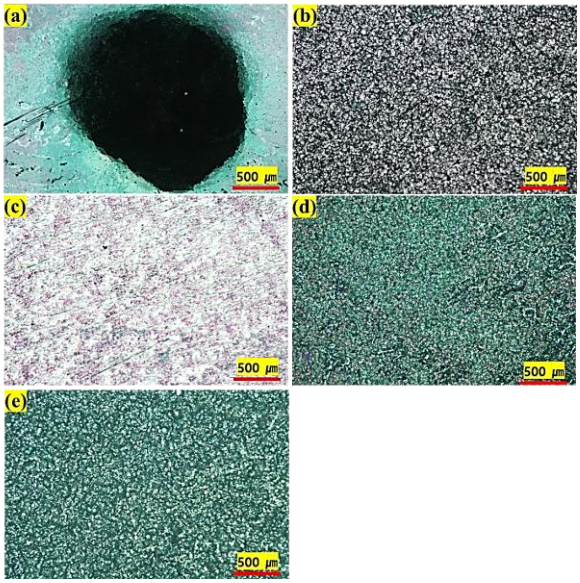

Fig. 7. OM images of the (a) SS304, (b) P-Ni, (c) P-Ti, (d) NP-Ni and (e) NP-Ti samples

3. Conclusions

In this study, the pitting corrosion behavior of cold-spray coatings were evaluated using an $FeCl_3$ immersion test. The SS304 substrate exhibited severe pitting after exposure, whereas the coated samples largely maintained their surface integrity. However, the polished Ni-coated sample displayed noticeable corrosion-induced defects, which were not observed in the polished Ti-coated sample. Due to their inherently high surface roughness, the as-deposited samples made it difficult to clearly identify corrosion features, necessitating further electrochemical experiments. Based on these results, the Ti-coated sample appears to be a promising candidate material for cold spray applications in interim storage canisters.

Future work will involve cross-sectional analysis of post-test samples using SEM to assess the extent of corrosion damage within the coatings. Additionally, electrochemical experiments will be performed to quantitatively compare the corrosion resistance of the two coating materials.

ACKNOWLEDGEMENT

This paper was supported by the 'Human Resources Program in Energy Technology' of the Korea Institute of Energy Technology Evaluation and Planning(KETEP), which was funded by the Ministry of Trade, Industry & Energy(MOTIE. Korea). (No. RS-2024-00398425) and by The Human Resources Development Project for HLW Management hosted by KORAD and MOTIE.

REFERENCES

[1] 1. R. Granaas, "SONGS Dry Cask Storage Inspection Operating Experience," EPRI ESCP Meeting, 2024
[2] Rodríguez, Martín A. "Anticipated degradation modes of metallic engineered barriers for high-level nuclear waste repositories." JOM 66.3 (2014): 503-525.
[3] Rokni, M. R., Nutt, S. R., Widener, C. A., Champagne, V. K., & Hrabe, R. H. (2017). Review of relationship between particle deformation, coating microstructure, and properties in high-pressure cold spray. Journal of thermal spray technology, 26(6), 1308-1355.
[4] Karasz, E. K., Montoya, T. D., Taylor, J. M., Ross, K. A., & Schaller, R. F. (2022). Accelerated corrosion testing of cold spray coatings on 304L in chloride environments. Frontiers in Metals and Alloys, 1, 1021000.